Indonesian Geotechnical Journal, August 2025, Vol 4 (2). Page 127-142
DOI: https://doi.org/10.56144/igj.v4i2.120
EISSN: 2829-7520
https://indonesian-geotechnical-journal.org/index.php/JGI/issue/archive

Water Retention Curve of Soil at Simpang Meo Region South Sumatra

Purnamawati[1], Herdian Gumay[2] and Nurly Gofar[3,*]
[1]Department of Civil Engineering, Graduate Program, Universitas Bina Darma, Jalan Jend. A. Yani No 3, Palembang, 30111, Indonesia; epur101112@gmail.com
[2]Doctoral Program, Department of Civil Engineering, Universitas Hasanuddin Jalan Poros Malino Km.6, Gowa, 92171, Indonesia; herdian.gumay@gmail.com
[3]Department of Civil Engineering, Graduate Program, Universitas Bina Darma, Jalan Jend. A. Yani No 3, Palembang, 30111, Indonesia; nurly_gofar@binadarma.ac.id
*Correspondence: nurly_gofar@binadarma.ac.id

SUBMITTED 20 August 2025 **REVISED** 29 August 2025 **ACCEPTED** 31 August 2025

ABSTRACT Steep slopes are typically formed on residual soil with deep groundwater levels; hence, the slopes are in the unsaturated zone. Therefore, in analyzing the stability of steep slopes, it is necessary to consider the properties of unsaturated soil. The main property of unsaturated soil is the Water Retention Curve (SWCC), which describes the relationship between matric suction and soil moisture content. Many methods are available to determine the SWCC of a soil, such as laboratory and field tests, as well as empirical equations. Laboratory testing is considered the best method for determining the SWCC. However, the laboratory work involved in the determination of SWCC is tedious; thus, several models have been developed by researchers to obtain SWCC. This study compares SWCC obtained based on the results of laboratory testing using an Osmotic Tensiometer assisted by soil shrinkage measurements using a 3-D scanner, and the SWCC obtained using the empirical equation proposed by Zapata for plastic soil based on the percentage of particles passing the No. 200 sieve and the soil plasticity index. The soil samples were retrieved from a location in the Simpang Meo region in South Sumatra. Air entry value for the SWCC was obtained both graphically and deterministically. Both methods resulted in a lower air entry value (AEV) for the Zapata equation as compared to the osmotic tensiometer test. A lower AEV indicates that lower suction is required for water to enter the soil pores. Therefore, analysis of rainfall infiltration and slope stability using SWCC curves estimated from the Zapata equation could result in later saturation of soil, hence a slightly higher factor of safety.

KEYWORDS Unsaturated Soil; Soil Water Characteristic Curve; Osmotic Tensiometer; Zapata Equation

1 INTRODUCTION

South Sumatra Province is located in the southern part of Sumatra Island, Indonesia. The region stretches from the east coast of Sumatra Island to the west bordering Bengkulu Province. The border between the two provinces is part of the Bukit Barisan Mountains, which were formed as a result of the collision between the Eurasian tectonic plate and the Indian-Australian Plate. Thus, the topography of the South Sumatra Province varies greatly, ranging from coastal morphology, lowlands, highlands, hills, and mountains. Based on the inventory data by the National Road Implementation Agency of South Sumatra Province (BPJNSS), eight (8) national roads in South Sumatra are prone to landslides, including National Road Section 15-021 connecting Simpang Sugihwaras (popularly known as Simpang Meo) and Muara Enim (Erlangga et al., 2024). Likewise, provincial roads connecting cities in these areas have experienced slope failures. For example, the provincial Road Section No. 049 between Simpang Meo and Semende in Semende Darat Laut sub-district, Muara Enim district, South Sumatra, frequently experiences slope failure, especially during rainy season. Based on the data collected by the Regional Disaster Management Agency (BPBD) of Muara Enim district, there have been 14 landslide incidents on Provincial Road Section No. 49 in the period of 2014 - 2023, including 7 incidents in 2022.

Steep slopes are typically formed on soils with deep groundwater levels, which keep them in the unsaturated zone. Unlike saturated soils, unsaturated soils exhibit negative pore water pressure, also referred to as suction (Rahardjo et al., 2016). Negative pore water pressure or suction from unsaturated soils provides additional shear strength as apparent cohesion. When water seeps into the soil, pore water pressure increases, and additional shear strength due to suction decreases or even disappears, making the slope more prone to failure (Rahardjo et al., 2019). The critical condition leading to slope failures is affected by several factors, including geology and hydrogeological factors, as well as geomorphology (Rahardjo et al., 2007). A field and numerical study conducted on the mountainous areas of South Sumatra concluded that slope failures occur due to high-intensity rain preceded by low-intensity rainfall (Gofar et al., 2025). The duration of the low-intensity rainfall defines the initial moisture condition of the soil, which is affected by the slope's geometry and the soil characteristics

To analyze the stability of steep slopes, it is necessary to consider the properties of unsaturated soil. The most important characteristic of unsaturated soil is its water retention capacity, which is usually presented in the form of a soil-water characteristic curve (SWCC). The SWCC defines a sigmoidal relationship between the soil moisture content and the soil suction ($u_a - u_w$) in a semi-logarithmic plot (Satyanaga et al., 2017). The soil water moisture is the amount of water within the pores of the soil; the higher the amount of water within these pores, the lower the soil suction and vice versa. Soil moisture can be displayed as gravimetric water content (ω), volumetric water content (θ), or degree of saturation (S_r). Field capacity affects the initial portion of the curve, while the grain size distribution controls the slope of the curve. The maximum amount of water that can enter the soil depends on the size of the soil pores (porosity). The soil suction has a range between nearly 0 for saturated conditions and 10^6 kPa (Rahardjo et al., 2019). The shape of the SWCC curve is characterized by the saturated volumetric water content (θ_s), the air entry value AEV (ψ_a), and the residual suction (ψ_r) at the residual water content (θ_r).

The SWCC plays a crucial role in explaining the hydraulic and mechanical characteristics of unsaturated soil, including water storage capacity, permeability coefficient, and strength properties (Fredlund et al., 2012). Mathematical and empirical models have been developed by researchers to correlate the soil's unsaturated permeability with suction (Tang et al., 2022). Likewise, unsaturated shear strength models were developed based on the SWCC curve by many researchers (Zhai et al., 2019).

Many researchers have developed methods to determine the SWCC of a soil. The most accurate method to obtain soil SWCC is by laboratory testing, including using hanging column, pressure plate, tempe cell, chilled mirror hygrometer, and centrifuge. The test procedure has been standardized in ASTM D6836. However, each method has limitations in terms of the range of suction power that can be measured. The combination of tempe cell (0 - 100 kPa) and pressure plate (100 - 1500 kPa) is the most common method used to determine SWCC in the laboratory (Satyanaga et al., 2023). In addition, the filter paper method (Likos & Lu, 2002) is generally used to obtain the SWCC curve through suction measurements at higher ranges (up to 1,000,000 kPa). The procedure is standardized in ASTM D5298. Rahardjo et al. (2021) introduced a new method to measure suction, the osmotic tensiometer method, which uses water-based polymers and can measure lower suction from 0.66 to 1500 kPa. This osmotic tensiometer tool can measure changes in suction quickly in the drying and wetting processes.

The procedure for determining points to create the SWCC curve in the laboratory is time-consuming and expensive, so there is usually lack of data points to form SWCC with full suction range. Several mathematical equations have been developed to form a good SWCC curve through the full suction range based on limited laboratory measurement points, for example, Gardner (1958), Brooks and Corey (1964), van Genuchten (1980), and Fredlund & Xing (1994).

In addition to laboratory testing, several correlations have been developed to estimate the SWCC. The equation proposed by Fredlund et al. (2002) is capable of estimating SWCC based on the grain size distribution of a soil particle size. Another method was developed by Zapata who uses the % of

particles passing the No. 200 sieve (w) and the soil plasticity index (PI) (Perera et al., 2005). Zapata's equation is more suitable for clay soil because it considers soil plasticity, while Fredlund's equation is only based on the distribution of soil particle size. Zapata equation has been tested on 190 soil samples consisting of 70 plastic soils and 120 non-plastic soils (Zapata et al., 2000). Data from this study clearly show that the AEV from the SWCC curve increases with increasing plasticity. Perera et al. (2005) stated that the error in predicting SWCC for plastic soil is as large as the difference in the curves made using the wPI between 10 and 30.

This article discusses the comparison of the soil water retention curve (SWCC) obtained from two methods. The first one is from laboratory testing using an Osmotic Tensiometer, assisted with shrinkage tests using a 3-D scanner, paired with Fredlund and Xing (1994) best-fit equation. The second one is the SWCC estimated using the Zapata equation (Perera et al., 2005). Soil samples were obtained from landslide that occurred on the road connecting Simpang Meo and Semende. The comparison is discussed based on the shape of the curve and SWCC parameters, namely air entry value (AEV or ψ_a). Note that in this study, the discussion is made for the drying curve only.

2 THEORETICAL BACKGROUND

2.1 Introduction to Soil Water Characteristics Curve (SWCC)

Soil water characteristic curve (SWCC) is a sigmoid function that relates soil moisture, presented as volumetric water content (θ), to matric suction (ψ). Matric suction (ψ) in unsaturated soil is the difference between pore air pressure (u_a) and pore water pressure (u_w) in the soil,

$$\psi = (u_a - u_w) \tag{1}$$

Volumetric water content (θ) is the ratio of the volume of water to the total volume of a soil sample. The θ is different from the gravimetric water content (ω) commonly used in geotechnical practice, which is the ratio of the weight of water to the weight of particles in a soil sample. Under saturated conditions

$$\theta = n\, S_r \tag{2}$$

where, n is the porosity and S_r is the degree of saturation. Volumetric water content in saturated soil is denoted as θ_s.

SWCC curve consists of three zones, namely the boundary effect zone, the transition zone, and the residual zone. The shape of the SWCC curve is characterized by the saturated volumetric water content (θ_s), the air entry value AEV (ψ_a), and the residual suction (ψ_r) at the residual water content (θ_r) (Figure 1). The boundary effect zone is the zone between suction = 0 and the air entry value (ψ_a) (Satyanaga et al., 2019). This zone represents the capillary fringe of groundwater in an unsaturated soil. The transition zone is the zone between the AEV and the residual condition. The air-entry value marks the suction where the air begins to penetrate and water begins to flow out of the largest pores, and desaturation occurs rapidly. The AEV can be determined graphically at the intersection of the tangent at the point of the maximum water content and the tangent at the point of the maximum gradient, called the inflection point. A deterministic approach to define AEV is proposed by Zhai & Rahardjo (2012). The slope of the quasi-linear portion of the curve describes the rate of change in the volume of water stored in the soil due to suction over a range of AEV values up to the suction corresponding to the residual water content. The rate of desaturation is controlled by the residual suction and permeability coefficient (Rahardjo et al., 2018). The residual water content (θ_r) is the volumetric water content of the soil at which further increases in suction do not produce a significant change in water content. The residual suction (ψ_r) at the residual water content (θ_r) can be determined graphically at the intersection of the tangent at the point of the inflection point and the tangent at the residual slope formed by data points.

The AEV value is influenced by the pore size distribution in the soil. Soils with large pores and particles of uniform size, such as sand, have relatively low AEV, because water can easily drain out under relatively small suction pressures compared to the high suction values required for silt or clay. The large pores in sandy soils cause all the water to drain out at small suctions, so the SWCC slope is steeper than in finer soils.

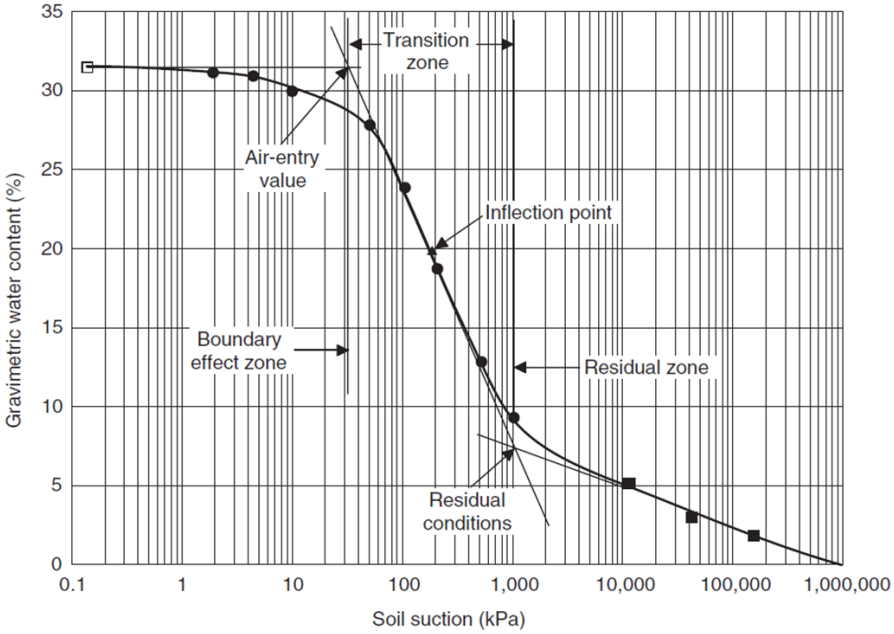

Figure 1 Drying SWCC curve with related parameters (Fredlund et al., 2012)

2.2 SWCC based on laboratory tests

The SWCC should be best established based on direct suction measurement in laboratory. However, the procedure for determining data points to create the SWCC curve is time-consuming and expensive, thus it is only feasible to obtain a few data points by direct suction measurement. Several mathematical equations have been developed to form a good SWCC curve and cover a large suction range. These equations have been reviewed by Sillers & Fredlund (2001) using a laboratory measurement database. They concluded that the Fredlund & Xing (1994) equation provides the closest match to the data set.

The Fredlund & Xing (1994) best-fitting equation is as follows:

$$\theta(\psi, a, n, m) = C(\psi) * \frac{\theta_s}{\left\{ln\left[e+\left(\frac{\psi}{a}\right)^n\right]\right\}^m} \quad (3)$$

where: θ_w is the volumetric water content (VWC), θ_s is the VWC at saturation, e is the base of the natural logarithm = 2.71828; a, n, and m are the corresponding parameters related to the air entry value in kPa (ψ_a), the slope at the inflection point, nt; $\psi = (u_a - u_w)$ is the matric suction (kPa); and $C(\psi)$ is the correction factor defined as follows:

$$C(\psi) = \frac{ln\left(1+\frac{\psi}{\psi_r}\right)}{ln\left[1+\left(\frac{1000000}{\psi_r}\right)\right]} + 1 \quad (4)$$

The parameter ψ_r is a fitting parameter related to the residual suction. However, Leong and Rahardjo (1997) recommend using $C(\psi) = 1$, and this was applied in this study as well. The characteristic values of the SWCC curve (i.e., the air entry value AEV, residual suction, and the slope of the SWCC

curve at the inflection point can be calculated using the equation of Zhai & Rahardjo (2012). The formula for determining the AEV value for correction factor $C(\psi) = 1$ is as follows:

$$\psi_{AEV} = a * 0.1^{\frac{3.72*1.31^{m+1}*(1-e^{-\frac{m}{3.67}})}{n*m*\ln(10)}} \quad (5)$$

while for $C(\psi) \neq 1$ is as follows:

$$\psi_{AEV} = a * 10^{\frac{\theta_i - \theta_s}{s_1}} \quad (6)$$

where the parameters *a, m* and *n* are the fitting parameters from Fredlund and Xing (1994). The parameter s_1 is the slope, θ_i the volumetric water content at the inflection point a_f and θ_s the saturated water content.

The results of the laboratory test yielded a SWCC curve for gravimetric water content. To obtain the SWCC for volumetric water content and degree of saturation, volume corrections are required. A shrinkage test was performed on the soil sample to define the volume of soil due to changing moisture content. Several equations were developed for generating shrinkage curves from gravimetric water content and measured volume changes (Leong & Wijaya, 2015), among others, is the Fredlund et al. (2002) comprehensive model for generating the shrinkage curves. This model represents only two linear segments in the shrinkage curve (Figure 2)

$$\theta = \frac{\omega \times Ws}{e} \quad (7)$$

where θ is the volumetric water content, ω is the gravimetric water content, W_s is the weight of soil particle (dry weight of sample), and e is the void ratio, which is a function of soil volume. The shrinkage curve could be developed based on the volume measurements during the SWCC test. Advanced scanning technology has been applied to measure the volume change of residual soil (Orazayeva et. al., 2024, Daramola et al., 2025).

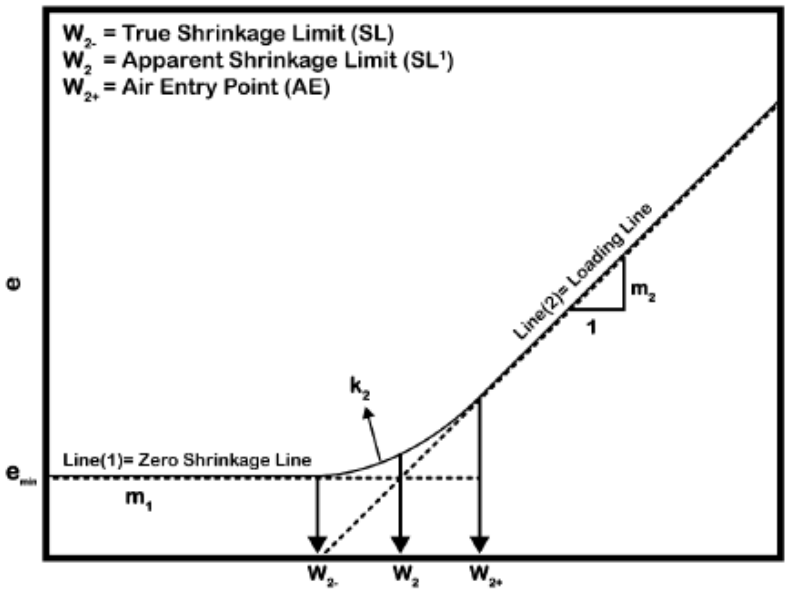

Figure 2 Shrinkage curve (Fredlund et al, 2002)

2.3 Empirical Correlation for Prediction of SWCC

To avoid time-consuming and expensive laboratory testing, several researchers have proposed mathematical models to estimate the SWCC curve. Fredlund et al. (2002) presented an estimation based on grain size distribution.

$$P_p = \frac{1}{ln\left(exp(1)+\left(\frac{g_a}{d}\right)^{g_n}\right)^{g_m}}\left(1-\left(\frac{ln\left(1+\frac{d_r}{d}\right)}{ln\left(1+\frac{d_r}{d_m}\right)}\right)^7\right) \quad (8)$$

where P_p is the percentage of particles passing a given diameter, d. g_a is the fitting parameter related to the start of the soil particle distribution curve, g_n is the fitting parameter related to the maximum slope of the soil particle distribution curve, g_m is the fitting parameter related to the shape of the soil particle distribution curve, d is the particle diameter (mm), d_r is the residual particle diameter (mm), and d_m is the minimum particle diameter (mm). This method, implemented in SoilVision software, is somewhat difficult to calculate manually but provides fairly reliable results for sand and silt. However, this method has several drawbacks for clay soils.

A mathematical model for plastic soil was proposed by Zapata (in Perera et al., 2005). This method is based on the grain size distribution (percentage of grains passing sieve No. 200, *w*) and the plasticity index (*PI*). These values are then used to calculate the parameters *a, n,* and *m* from the Fredlund and Xing (1994) equation to describe the SWCC of plastic soil:

$$wPI = PI * P_{200} \text{ (in decimal)} \quad (9)$$

$$a = 32.835\{ln(wPI)\} + 32.438 \quad (10)$$

$$n = 1.421(wPI)^{-0.3185} \quad (11)$$

$$m = -0.2154\{ln(wPI)\} + 0.7145 \quad (12)$$

ψ_r = 500 kPa (13)

3 METHODOLOGY

3.1 Location of Landslide and Soil Sampling

The soil used for the laboratory test was obtained from a landslide location in the Padang Bindu Village, Pahang Enim District, Muara Enim Regency (Simpang Meo), shown in Figure 3. This location is traversed by Provincial Road No. 49, which connects the Lahat regency and Sugihwaras subdistrict.

Figure 3. Location of slope landslide and soil sampling (Google Earth)

The landslide occurred at approximately 08:00 WIB on February 1, 2023, at the coordinates of 4º 03'51"S, 103º 39'37"E. The landslide caused an interruption of traffic on the Provincial Road for several hours. Measurements taken at the time of the landslide indicated that the length of the landslide was approximately 15 meters and the depth of the sliding plane was 1 – 2 meters. The landslide occurred after heavy rainfall at the location. The total amount of rainfall in the ten days before the landslide was 98 mm. The conditions at the time of the landslide and after initial handling are shown in Figure 4. The reconstruction of the sliding plane, shown in Figure 5, supports that the failure was induced by rainfall (shallow surface failure).

Figure 4 Landslide at Simpang Meo: after the landslide on 1 February 2023 (left); after initial treatment (right)

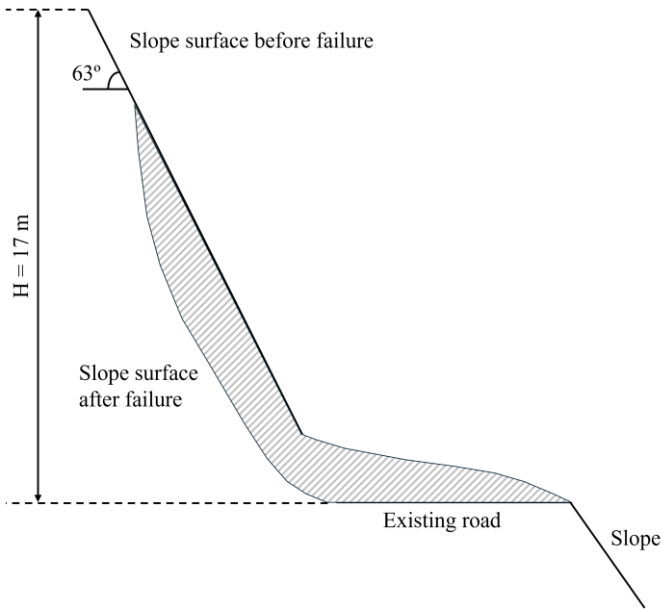

Figure 5 Reconstruction of the sliding plane

3.2 Initial Laboratory Testing

As much as 50 kg of disturbed sample was retrieved from a depth of 2 m near the landslide site. Index property tests were conducted based on relevant ASTM standards. Specific gravity testing was conducted following ASTM D854-02. Grain size distribution was determined based on ASTM D422. Atterberg limits (liquid limit, plastic limit, and plasticity index) tests were carried out based on ASTM D4318-00.

3.3 SWCC Test

SWCC testing was performed in a laboratory using an Osmotic Tensiometer (Rahardjo et al., 2021), which operates on the principle of osmotic pressure differences across a semipermeable membrane, to measure soil water potential in porous media. The equipment consists of a high-concentration osmotic solution that generates osmotic pressure through a pressure sensor and a porous ceramic tip. When inserted into the soil, water moves across the membrane according to the difference in water potential between the osmotic solution inside the tensiometer and the surrounding soil (Liu et al., 2021). Before measuring the soil, the sensor needs to be calibrated at ambient temperature against a reference temperature of 25°C. Osmotic tensiometer testing was conducted in a controlled laboratory environment. Humidity levels were kept constant at a temperature range of 19° to 25°C.

The equipment setup is shown in Figure 6. All components are assembled in a vertical position on a digital balance. The sensor cable is secured using a cable support and connected to a computer. Measurements from the osmotic tensiometer and balance are automatically recorded by the computer at predetermined time intervals, allowing the data to be accessed at any time during the testing process for analysis. The tests were performed on a reconstituted and compacted specimen 90 mm in diameter and 30 mm in height. The soil specimen is placed in the chamber and saturated with distilled water. The saturation process is considered complete when no significant changes are observed in the soil specimen. Then, the sample is placed on a support frame and positioned on a stand equipped with a restrictive ring to position the osmotic tensiometer into the soil specimen. The mass of the specimen is measured before and after the drying process is complete. The water content of the soil specimen can be calculated based on the dry mass of the soil.

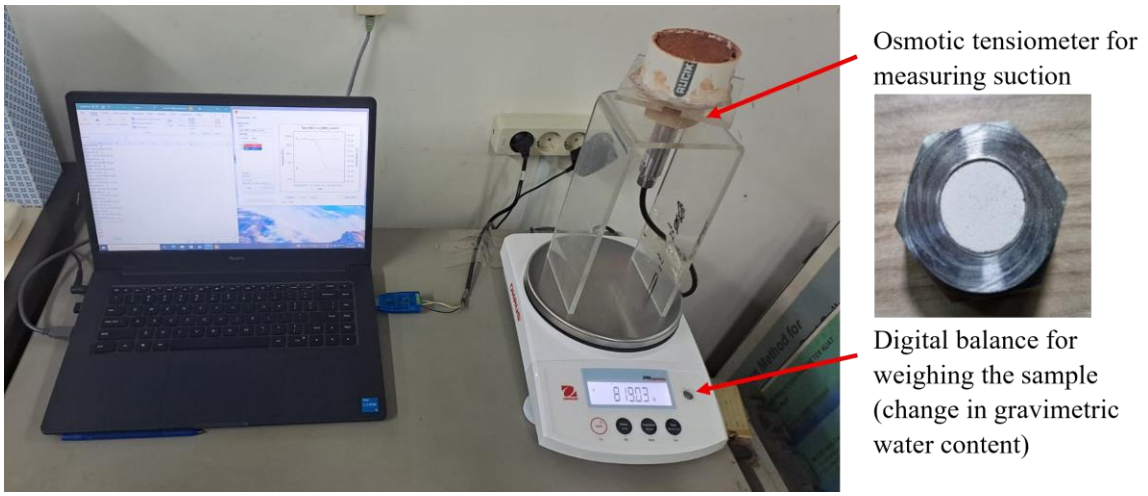

Figure 6: Equipment setup and the Osmotic Tensiometer for measuring suction

In this study, the measurement interval was set to five minutes interval, and test data were collected daily for further analysis. Mass measurements recorded by the balance were used to determine the water content of the soil specimens, while suction measurements were obtained using an osmotic tensiometer. Based on this study, the test duration generally ranged from 5 to 14 days, depending on the type of soil being tested.

The results of this test generated a SWCC curve for gravimetric water content. To obtain the SWCC for volumetric water content and degree of saturation, volume corrections are required. Sample volume corrections were made by measuring the sample volume for each application. Measurements were made using a three-dimensional scanner.

A 3D scanner (Figure 7) is used to capture 360° views of soil specimens due to their irregular shapes. The camera generates a comprehensive digital representation of the physical object based on the distances between points captured over a specific scanning distance.

Figure 7 The 3 - D Scanner for measuring volume change

3.4 Data Processing

SWCC test using an Osmotic Tensiometer produces a series of data to define the SWCC in terms of gravimetric water content. Then the volume of soil sample for each suction was calculated based on the shrinkage curve derived based on volume change data obtained from a 3-D scanner and the Fredlund et al. (2002) equation. The volume change in terms of void ratio was used to calculate the volumetric water content using equation (6); thus, the SWCC can be plotted in terms of volumetric water content. The Fredlund and Xing (1994) model is used to connect the test points to produce a smooth curve with a range between 0 and 10^6 kPa. Microsoft Excel is used to obtain the curve based on laboratory data and mathematical equations. The values of *a, n,* and *m* in the Fredlund & Xing equation are obtained for the smallest error value. Then the AEV value can be calculated using the equation of Zhai et & Rahardjo (2012).

3.5 SWCC Estimation Based on Index Properties

The data from the sieve analysis test results and Atterberg limits are used to form the SWCC curve using the Zapata equation (Perera et al., 2005). The Microsoft Excel program is also used to obtain a curve based on the data of particles passing through sieve no. 200 (P_{200}) and the plasticity index. The values of *a, n, and m* are calculated using Equations 9 – 14. Then the AEV value can also be calculated using equation 5 or graphically using the inflection point for the correction factor $C(\psi) = 1$.

4 RESULTS AND DISCUSSION

4.1 Index Properties and Soil Classification

The results of the physical properties and soil classification tests are shown in Table 1. The laboratory test results indicate that the soil can be classified as silt or clay with low plasticity (CL). Based on Table 1, the soil contains 46.01% fine particles (passing the No. 200 ASTM sieve), consisting of 26.92% silt and 19.09% clay. The liquid limit is 34.09%, while the soil plasticity index is 12.52%. The particle size distribution and the soil plasticity are shown in Figures 8 and 9.

Table 1. Soil properties

Soil Properties	Unit	
Specific Gravity (G_s)		2.69
Density (ρ)	g/cm^3	1.73
Porosity (θ_n)		0.56
Sieve Analysis		
Passing No 200 (<75 m)	%	46.01
Clay content (<2m)	%	19.09
Atterberg Limits		
Liquid Limit	%	34.09
Plasticity index	%	12.52
Soil Classification		CL

4.2 Results of SWCC Test Using Osmotic Tensiometer

Laboratory SWCC testing was conducted using an Osmotic Tensiometer. Suction measurements were conducted for 5 days (March 24 – 31, 2024), resulting in 1250 data points with a suction range between 9.5 kPa and 650 kPa. The test results in the form of a gravimetric curve are shown in Figure 8.

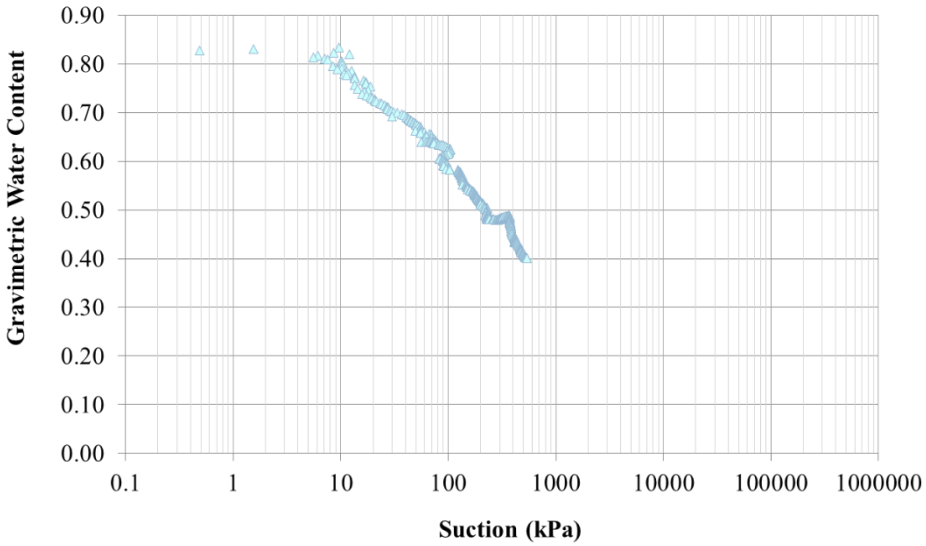

Figure 8 Laboratory test data in terms of gravimetric water content

Shrinkage testing was conducted to obtain shrinkage curve (SC) which is required to consider two independent processes of volume change and degree of saturation change involved in the obtain the SWCC in terms of volumetric water content. The curve formed by the test points was paired with the Fredlund et al. (2002) equation as follows:

$$e(w) = a_{sh}\left[\frac{w^{c_{sh}}}{(b_{sh})^{c_{sh}}} + 1\right]^{\frac{1}{c_{sh}}} \quad (14)$$

where: $e(w)$ is the void ratio of the soil at a gravimetric water content, a_{sh} is the minimum void ratio (emin); b_{sh} is the slope of the line of tangency, and c_{sh} represent the curvature of the shrinkage curve.

The duration of the shrinkage test was 10 days (June 3 – 13, 2024), resulting in a shrinkage curve with fitting parameters a_{sh} = 1.194, b_{sh} = 44.387, c_{sh} = 4.254 as shown in Figure 9.

From the results of the Osmotic Tensiometer test and the results of the shrinkage test, the SWCC curve for volumetric water content can be drawn as shown in Figure 10. The curve is fitted with the Fredlund and Xing (1994) equation with a correction factor of $C(\psi) \neq 1$. The resulting parameters are a = 300, n = 1, m = 1.1, θ_s = 0.68, C_r = 500. The AEV value is calculated using Equation 6 for $C(\psi) \neq 1$, resulting in an AEV = 32 kPa. The AEV value obtained graphically, based on an inflection point at ψ = 700kPa, was 72 kPa.

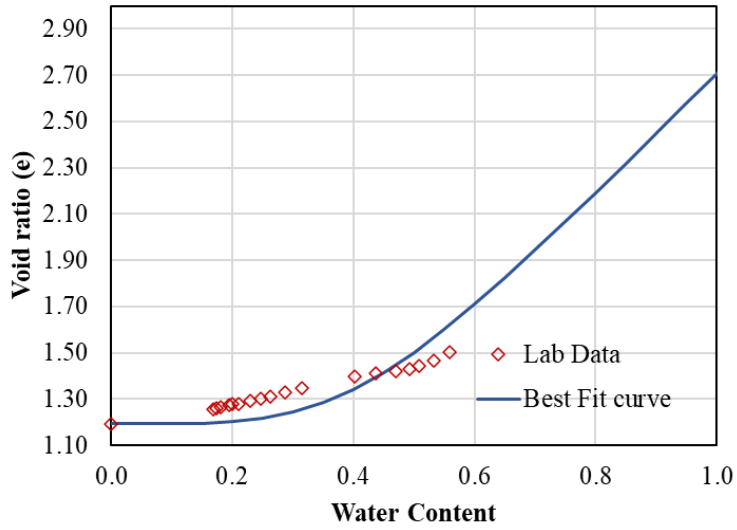

Figure 9 Results of Shrinkage Test

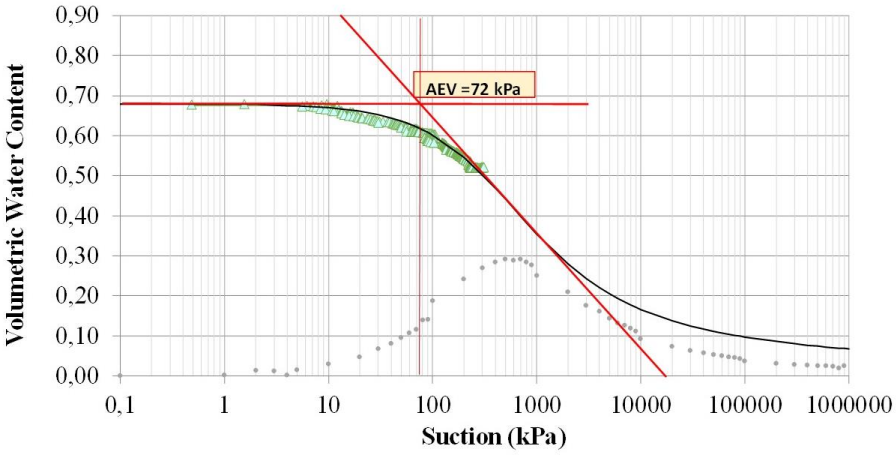

Figure 10 SWCC of the soil at the Landslide location in terms of volumetric water content

4.3 SWCC Estimation Using Zapata Equation

The SWCC curve estimation using the Zapata equation is made using equations 9 – 13. The values of a, n, and m are calculated based on the product of the percentage of particles passing through sieve No. 200 and the plasticity index, namely wPI = 5.76, resulting in a = 89.933, n = 0.814, m = 0.337, volumetric water content at saturated conditions θ_s = 0.68 and C_r = 500. The AEV value calculated

using equation 5 with the assumption of $C(\psi) \neq 1$, giving an AEV value of 16 kPa, while graphically using the inflection point at 1258 kPa, obtaining an AEV value of 57 kPa.

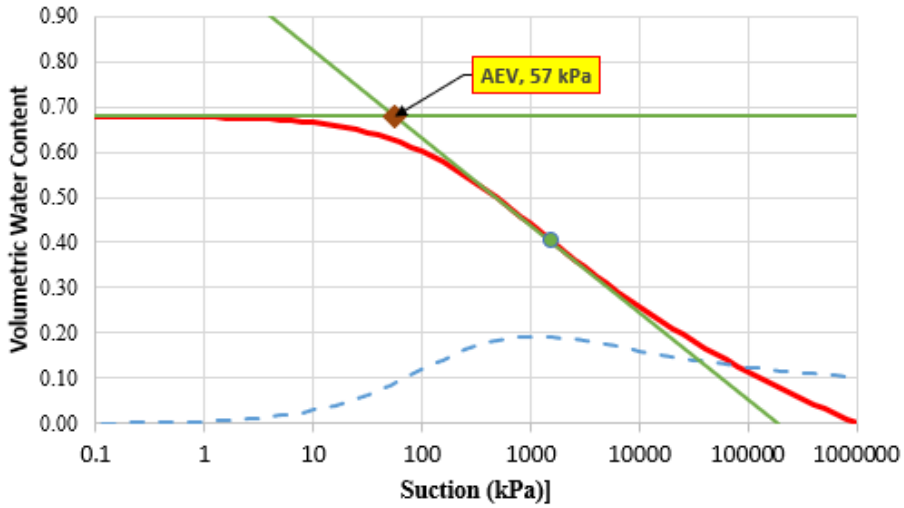

Figure 11 SWCC estimated using Zapata equations

4.4 Discussion

From Figures 10 and 11, it can be seen that the AEV value, with the assumption of $C(\psi) \neq 1$, obtained from the Zapata equation, is lower than that obtained from the Fredlund & Xing equation paired with data acquired from laboratory testing using an Osmotic Tensiometer. Figure 12 shows that the shape of SWCC using the Zapata model is flatter, resulting in higher suction at the inflection point (1258 kPa) as compared to the inflection point obtained from Fredlund and Xing's equation (700 kPa). The higher inflection point resulted in a lower AEV value (57 kPa vs. 72 kPa). Likewise, the AEV value obtained deterministically using Equation 5 provides a lower AEV value for the Zapata method (13 kPa) as compared to the best-fitting equation for data points obtained in the laboratory test (32 kPa). A lower AEV indicates that lower suction is required for water to enter the soil pores. Therefore, analysis of rainfall infiltration and slope stability using SWCC curves estimated from the Zapata equation could result in later saturation of soil, hence a slightly higher factor of safety. Table 2 provides a summary of SWCC parameters obtained using both methods.

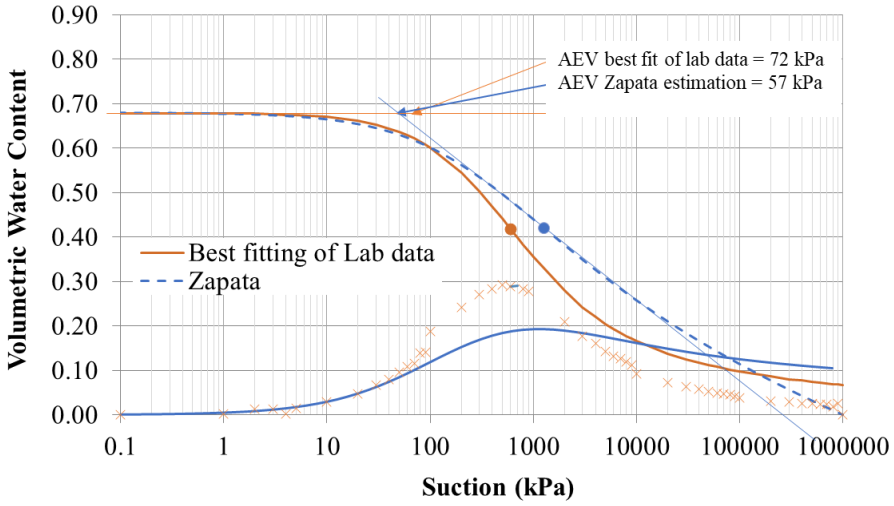

Figure 12 Comparison of SWCC obtained based on laboratory data with that obtained using Zapata method

Table 2. SWCC parameters obtained using laboratory data and the estimation method using Zapata equation

SWCC Parameters	Based on Lab data	Zapata estimation method
SWCC curve	curvy	flatter
Inflection point	700 kPa	1258 kPa
AEV deterministic	32 kPa	13 kPa
AEV graphic	72 kPa	57 kPa

5 CONCLUSIONS

The following conclusions could be derived from the analysis of slope failure in Simpang Meo on 1st February 2023 and the unsaturated soil characteristics at the site:

1. Based on the reconstruction of the sliding plane, the position of the groundwater table, and the rainfall conditions before failure, the slope failure was triggered by rainfall.
2. The SWCC curve estimated using the Zapata equation differs slightly from the SWCC curve obtained from testing using an Osmotic Tensiometer coupled with the Fredlund & Xing equation. The Zapata curve is flatter, resulting in higher suction at the inflection point, therefore a lower AEV value both graphically and deterministically.
3. A lower AEV indicates that lower suction is required for water to enter the soil pores. Therefore, analysis of rainfall infiltration and slope stability using SWCC curves estimated from the Zapata equation could result in later saturation of soil, hence a slightly higher factor of safety

DISCLAIMER

The authors declare no conflict of interest.

ACKNOWLEDGMENT

The authors acknowledge the assistance given by Dr. Abdul Halim Hamdany and Mr. Yudi Harianto in the laboratory testing and processing of data used in this paper.

REFERENCES

ASTM D4318-00. Standard Test Methods for Liquid Limit, Plastic Limit, and Plasticity Index of Soils; ASTM International: West Conshohocken, PA, USA, 2000.

ASTM D854-02. Standard Test Methods for Specific Gravity of Soil Solids by Water Pycnometer; ASTM International: West Conshohocken, PA, USA, 2002.

ASTM D2487-00. Standard Practice for Classification of Soils for Engineering Purposes, Unified Soil Classification System; ASTM International: West Conshohocken, PA, USA, 2000.

ASTM D6836-16. Standard Test Methods for Determination of the Soil Water Characteristic Curve for Desorption Using Hanging Column, Pressure Extractor, Chilled Mirror Hygrometer, or Centrifuge. ASTM International: West Conshohocken, PA, USA, 2000.

ASTM D5298-16. Standard Test Method for Measurement of Soil Potential (Suction) Using Filter Paper. ASTM International: West Conshohocken, PA, USA, 2000.

Zuhri, A., 2023. *Ruas Jalan Simpang Meo-Semende di Muara Enim Tertimbun Longsor, Arus Lalulintas Lumpuh Berapa Jam* [In Indonesian, Online]. Available at: https://palembang.tribunnews.com/2023/02/01/ruas-jalan-simpang-meo-semende-di-muara-enim-tertimbun-longsor-arus-lalulintas-lumpuh-beberapa-jam?page=1 [Accessed 31 August 2025]

Brooks, R. H., and Corey, A.T., 1964. Hydraulic properties of porous media. *Hydrology Papers, Colorado State University*, 24, p. 37.

Daramola, A. M., Satyanaga, A., Adejumo, B. D., Kim, Y., Qian, Z., & Kim, J., 2025. Real-Time Scanning Curve of Soil–Water Characteristic Curve for Sustainability of Residual Soil Slopes. *Sustainability*, 17(5), p. 1803. https://doi.org/10.3390/su17051803

Erlangga, S., Bulkin, F. & Gofar, N., 2024. Mapping of Risk Levels and Types of Slope Failure in South Sumatra. *Rekayasa Sipil*, 18(1), pp. 66-71. https://doi.org/10.21776/ub.rekayasasipil.2024.018.01.04

Fredlund, D. G., Rahardjo, H., & Fredlund, M. D., 2012. *Unsaturated Soil Mechanics in Engineering Practice*. Hoboken, New Jersey: Wiley.

Fredlund, M. D., Wilson, G. W. & Fredlund, D. G., 2002. Representation and estimation of the shrinkage curve. *Proceedings 3rd International Conference on Unsaturated Soils (UNSAT 2002)*.

Fredlund, M. D., Wilson, G. W., & Fredlund, D. G., 2002. Use of the grain-size distribution for estimation of the soil-water characteristic curve. *Canadian Geotechnical Journal*, 39(5), pp. 1103-1117. https://doi.org/10.1139/t02-049

Fredlund, D. G., & Xing, A., 1994. Equations for the soil-water characteristic curve. *Canadian Geotechnical Journal*, 31(3), pp. 521 - 532. https://doi.org/10.1139/t94-061

Gardner, W. R., 1958. Some steady-state solutions of unsaturated moisture flow equations with applications to evaporation from a water table. *Soil Science*, 85(4), pp. 228–232.

van Genuchten, M. Th., 1980. A closed-form equation for predicting the hydraulic conductivity of unsaturated soils. *Soil Science of America*, 44, pp. 892-898. https://doi.org/10.2136/sssaj1980.03615995004400050002x

Gofar, N., Harianto, Y., & Purnama Sari Dewi, A., 2025. Identification of Rainfall Scenario Triggering Slope Failures in Pagar Alam and its Surrounding Area. *Media Komunikasi Teknik Sipil*, 30(2), pp. 256-264. https://doi.org/10.14710/mkts.v30i2.62372

Leong, E. C., & Rahardjo, H., 1997. A review of soil-water characteristic curve equations. *Journal of Geotechnical and Geoenvironmental Engineering (ASCE)*, 123(12), pp. 1106 - 1117. https://doi.org/10.1061/(ASCE)1090-0241(1997)123:12(1106)

Leong, E. C. & Wijaya, M., 2015. Universal soil shrinkage curve equation. *Geoderma*, 237–238, pp. 78-87. http://dx.doi.org/10.1016/j.geoderma.2014.08.012

Likos, W. J., & Lu, N., 2002. Filter Paper Technique for Measuring Total Soil Suction. Transportation Research Record: Journal of the Transportation Research Board, 1786(1), pp. 120-128. https://doi.org/10.3141/1786-14

Liu, H., Rahardjo, H., Satyanaga, A. & Du, H., 2021. Use of synthesised polymers for the development of new osmotic tensiometers. *Géotechnique*, 73, pp. 544-552. https://doi.org/10.1680/jgeot.21.00108

Orazayeva, S., Satyanaga, A., Kim, Y., Rahardjo, H., Qian, Z., Moon, S.-W., & Kim, J., 2024. Advanced Scanning Technology for Volume Change Measurement of Residual Soil. *Applied Science*, 14, 10938. https://doi.org/10.3390/app142310938

Perera, Y. Y., Zapata, C. E., Houston, W. N., & Houston, S. L., 2005. Prediction of the Soil-Water Characteristic Curve Based on Grain-Size-Distribution and Index Properties. *Proceedings of GeoFrontiers 2005*. https://doi.org/10.1061/40776(155)4

Rahardjo, H., Shen, Y., Tsen-Tieng, D. L., Ramos-Rivera, J., Nong, X., & Hamdany, A. H., 2021. New Osmotic Tensiometer Development. *Geotechnical Testing Journal*, 44(3), pp. 722–740. https://doi.org/10.1520/GTJ20190451

Rahardjo, H., Satyanaga, A., Gofar, N., Zhai, Q., Leong, E. C., Kew, J. H., Wang, C. L., & Wong, J. L. H., 2019. Geobarrier System for Slope Protection against Rainfall-induced Slope Failure. *International Journal of Geoengineering Case Histories*, 5(1), pp. 28-43 http://dx.doi.org/10.4417/IJGCH-05-01-03

Rahardjo, H., Gofar, N., & Satyanaga, A., 2018. Effect of Concrete Waste Particles on Infiltration Characteristics of Soil. *Environmental Earth Science*, 77(9), pp. 347-359. https://doi.org/10.1007/s12665-018-7530-3

Rahardjo, H., Satyanaga, A. & Leong, E. C., 2016. Effects of rainfall characteristics on the stability of tropical residual soil slope. *Proceedings of E-UNSAT 2016*, E3S Web of conferences 9, Sep 2016, 15004, pp. 1-6, https://doi.org/10.1051/e3sconf/20160915004

Rahardjo, H., Santoso, V. A., Leong, E. C., Ng, Y. S., Tam, C. P. H., & Satyanaga, A., 2013. Use of recycled crushed concrete and Secudrain in capillary barriers for slope stabilization. *Canadian Geotechnical Journal*, 50(6), pp. 662-673. https://doi.org/10.1139/cgj-2012-0035

Rahardjo, H., Ong, T. H. Rezaur, R. B., and Leong, E. C., 2007. Factors Controlling Instability of Homogeneous Soil Slopes under Rainfall Loading. *Journal of Geotechnical and Geoenvironmental Engineering (ASCE)*, 133(12), pp. 1532 – 1543. DOI: https://doi.org/10.1061/(ASCE)1090-0241(2007)133:12(1532)

Satyanaga, A., Rahardjo, H., Koh, Z. H., & Mohamed, H., 2019. Measurement of a Soil-water Characteristic Curve and Unsaturated Permeability using the Evaporation Method and the Chilled-Mirror Method. *Journal of Zhejiang University-SCIENCE A*, 20(5), pp. 368-375. https://doi.org/10.1631/jzus.A1800593

Satyanaga, A., Mohammad, A. S., Ibrahimi, A. B., & Wijaya, M., 2023 Direct and indirect methods in determination of water retention curve of residual soils, in Zhussupbekov, A., Sarsembayeva, A. & Kaliakin, V. N. (ed.), *Smart Geotechnics for Smart Societies*, pp. 363-371

Satyanaga, A., Zhai, Q., & Rahardjo, H., 2017 Estimation of Unimodal Water Characteristic Curve for Gap-graded Soil. *Soils and Foundations*, 57(5), pp. 789-801. https://doi.org/10.1016/j.sandf.2017.08.009

Sillers, W. S., & Fredlund, D. G., 2001. Statistical assessment of soil-water characteristic curve models for geotechnical engineering. *Canadian Geotechnical Journal*, 38(6), pp. 1297 - 1313. https://doi.org/10.1139/t01-066

Tang, L., Tian. G., Dai, G., Zhai, Q., Rahardjo, H., & Satyanaga, A., 2022. Effect of threshold suction on the prediction of the permeability function by using the statistical method. *Results in Engineering*, 14, 100456. https://doi.org/10.1016/j.rineng.2022.100456

Wijaya, M., Lim, A., Rahardjo, P. P., Satyanaga, A., Hamdany, A. H., & Adiguna, G. A., 2024. Determination of soil–water characteristic curves by using a polymer tensiometer. *Journal of the Mechanical Behavior of Materials*, 33(1), 20240007. https://doi.org/10.1515/jmbm-2024-0007

Zapata, C. E., Houston, W. N., Houston, S. L., & Walsh, K. D. 2000. Soil-WaterCharacteristic Curve Variability. *Proceedings of Sessions of Geo-Denver 2000*, Denver: ASCE Geo-Institute, pp. 84-124

Zhai, Q. & Rahardjo, H., 2012. Determination of Soil-Water Characteristic Curve Variables. *Computer and Geotechnics*, 42, pp. 37-43. https://doi.org/10.1016/j.compgeo.2011.11.010

- This page is intentionally left blank -